Journal of Power Sources 232 (2013) 357–369

Contents lists available at SciVerse ScienceDirect

Journal of Power Sources

journal homepage: www.elsevier.com/locate/jpowsour

Review

# Review and analysis of nanostructured olivine-based lithium recheargeable batteries: Status and trends

K. Zaghib [a,*], A. Guerfi [a], P. Hovington [a], A. Vijh [a], M. Trudeau [a], A. Mauger [b], J.B. Goodenough [c], C.M. Julien [d]

[a] Institut de Recherche d'Hydro-Québec (IREQ), 1800 Bd Lionel-Boulet, Varennes, Québec, Canada J3X 1S1
[b] Université Pierre et Marie Curie-Paris6, Institut de Minéralogie et Physique de la Matière Condensée (IMPMC), 4 place Jussieu, 75005 Paris, France
[c] The University of Texas at Austin, Austin, TX 78712, USA
[d] Université Pierre et Marie Curie-Paris 6, Physicochimie des Electrolytes, Colloïdes et Sciences Analytiques (PECSA), 4 place Jussieu, 75005 Paris, France

## HIGHLIGHTS

- The Li$MPO_4$ ($M$ = Fe, Mn) performance as a cathode of Li-ion batteries is reviewed.
- The state of the art in the understanding of these compounds is reported.
- Misunderstanding of size effects down to the nanoscale are outlined.
- The improvements expected from the nano-structure are discussed.
- The most recent results and novel routes are to improve the performance of Li-ion batteries in the near-future are discussed.

## ARTICLE INFO

*Article history:*
Received 21 October 2012
Received in revised form
21 December 2012
Accepted 24 December 2012
Available online 9 February 2013

Karim Zaghib presented this paper in honor of Dr. Goodenough's 90th birthday [117].

*Keywords:*
Nanostructed material
Olivines
Cathode
Li-ion
Li rechargeable batteries

## ABSTRACT

$LiFePO_4$ has emerged as the winning cathode material for a new generation of Li-ion batteries that are increasingly used for hybrid and electric vehicles, due to its remarkable electrochemical properties. The present review gives the state of the art in the understanding of the properties of this material and the other members of the same family. We discuss the effects of the decrease of the size of the particles down to circa 20 nm; some of them have been misunderstood or are still open questions. All of them are important to determine the trends in the research and development on this family of materials in the future. The cells' properties are also reviewed with both the graphite and more recently the $Li_4Ti_5O_{12}$ anodes, the last one providing outstanding performance in terms of cycling life and power that make them promising not only for electric vehicles, but also to solve for intermittence locally in smart grids.
© 2013 Elsevier B.V. All rights reserved.

## 1. Introduction

Sony was the first corporation to commercialize a Li-ion battery [1]. Equipped with a $LiCoO_2$ cathode, it was extensively used for portable applications. The toxicity, and high cost of Co, plus the safety hazard associated with battery fires due to poor thermal stability of $LiCoO_2$ and other lamellar compounds of the same family [2], have been the motivation for the research of novel cathode elements. The spinel $LiMn_2O_4$ was proposed in the late 1980s [3]. However, fading problems and dissolution of manganese prevent the material from being used without additional traps of manganese, namely a lamellar compound that introduces an unstable element again. More recently, $LiFePO_4$ (LFP) that belongs to the olivine group has emerged as the critical cathode material of the world's new generation of rechargeable batteries for computers, power tools, mobility products, consumer electronics, cell phones, large-scale power storage applications, and hybrid electric vehicles (HEVs) [4]. Due to the economical impact, over 1200 patents have been issued or applied for in the area of Li$MPO_4$ ($M$ = transition metal of the first row) cathodes [5] since the first patent [6], and the production of $LiFePO_4$ is growing exponentially. It is the stable and safe olivine structure of LFP material that makes

* Corresponding author.
*E-mail address:* zaghib.karim@ireq.ca (K. Zaghib).

0378-7753/$ – see front matter © 2013 Elsevier B.V. All rights reserved.
http://dx.doi.org/10.1016/j.jpowsour.2012.12.095

$LiFePO_4$ favorable in lithium batteries. At contrast with the other cathode materials with layered and spinel structure, the framework of which may transform or release oxygen, the strong P–O bonds in LFP prevent the explosion of the battery, as the framework itself does not explode even in case of a short circuit of a lithium battery. Getting rid of the problems with runaway overheating and out gassing, LFP-based batteries do not need as intense battery monitoring systems (BMS) as the other Li-ion batteries. Having no competitor in terms of safety [7,8], cycling life and power [9], LFP cathodes are devoted to hybrid vehicles as the critical market.

The cathode is the main element that determines the performance of Li-ion batteries. The anode materials, however, also have some impact. Before Li-ion batteries, metallic Li has been used. There are problems, however, associated with it: *e.g.* corrosion of Li by reaction with the electrolyte, safety aspects caused by dendrite formation short-circuiting a cell, thermal runaway, poor power. The substitution of Li-metal by an insertion material has solved this problem [10], and the batteries are referred to as Li-ion cells [11]. In these cells, an insertion electrode, usually graphite [12] replaces the Li metal anode that has been abandoned for any automotive application (except by the polymer battery by Batscap in France). A review of various nanostructured materials used for the cathodes and anodes has been published recently [13]. Due to the importance of $LiFePO_4$, the present review only focuses on the olivine family of nanostructured cathodes. In the same way, we also limit the review to the anode materials associated with this cathode, namely graphite, and more recently the spinel $Li_4Ti_5O_{12}$.

The performance of $LiFePO_4$ reached today is the result of intensive research to reduce the size of the particles to the nanoscale. It is important, however, to specify what "nano" means here. In electronics, for instance, it signifies particles that are so small the electronic or the magnetic properties are modified by quantum confinement of the electrons. It means particles smaller than 10 nm. In the physics and electrochemistry of the cathode elements of Li-ion batteries, however, the term is used to signify particles so small that their properties depend importantly on surface effects. Typically, the surface layer is about 3 nm thick, so that particles are labeled "nano" in the literature if their size is smaller than 100 nm, and usually in the range 20–100 nm. So far, there has been little interest to synthesize smaller particles because too small particles have been reported to reduce the tap density [14] and they are much more difficult to handle in making electrodes for the industry of Li-ion batteries. It turns out that some size effects on the physical and chemical properties of the particles have been observed in this "nano" range, as we shall see later in this review, but they were not necessarily expected and may not be totally understood. Still, there have been many efforts through the years to decrease the size of the particles from a few microns to this "nano" range, for several reasons. One is the increase of the effective contact area of the powder with the electrolyte. A larger effective contact surface with the electrolyte means a greater probability to drain $Li^+$ ions from the electrode, which increases the power density of the cell. A smaller particle size also reduces the Li diffusion length to the interior of the particle, which leads to a greater capacity at higher charge/discharge rates and therefore to a larger power density. In addition, the small electronic conductivity of the olivine particles that results from a two-phase $FePO_4/LiFePO_4$ reaction has led to coating of the particles with a thin layer that is conductive of both electrons and Li, usually an amorphous carbon layer [15]. Decreasing the particle size reduces the length of the tunneling barrier for electrons to travel from/to the surface layer or to/from the core of the particle, which also increases the power density. The coat may also decrease the activation energy for $Li^+$ transfer across the electrode/electrolyte interfaces.

Although $LiFePO_4$ has the best electrochemical performance, the members of the family include $LiMPO_4$ with $M$ = Mn, Ni, Co. The $Mn^{3+}/Mn^{2+}$ redox potential *vs.* $Li^+/Li$ is 4.1 V, larger than that of $Fe^{3+}/Fe^{2+}$ in the olivine lattice. Advances on the nanoparticles involving $LiMnPO_4$ will also be reviewed. The working potentials of the cells with Ni and Co, however, are outside the electrolyte window. These compounds are thus of little interest until one finds the possibility to make a battery working at 5 V, a problem that has been under extensive investigation for many years, but is still unsolved; therefore they will not be considered here.

A common feature to all olivine materials is their poor electronic conductivity. Therefore, bare particles have very poor electrochemical properties. Therefore, the active element of the cathode is always a nano-composite C-$LiMPO_4$ that designates the nanoparticle with its carbon coat.

There are many ways to synthesize olivine materials. They have already been extensively reviewed recently [16,17]; therefore, we simply refer to these works for synthesis information. This review is focused on the effect of the particle size and morphology on their electrochemical properties. The role of the nano-painting is also reported, and the novel advanced and more complex nano-olivine composites are reviewed at the end.

## 2. The Gibbs' phase rule

An intercalation electrode, considered as solution of guest A in the host lattice ⟨H⟩ has a potential variation for a given redox couple in the host given by the classical thermodynamic law:

$$V(x) = -\frac{1}{zF}\frac{\partial(\Delta G)}{\partial x} + \text{constant}, \tag{1}$$

where $\Delta G$ denotes the variation in the Gibbs energy of the system, $x$ the composition, $z$ the number of electrons involved and $F$ the Faraday's constant. The electrode potential is a function of the composition $x$ in $\langle A_xH\rangle$.

In a closed system at equilibrium, the Gibbs' phase rule states that the relation between the number of degrees of freedom, $f$, and the number of independent components, $c$, is given by

$$f = c - p + n, \tag{2}$$

where $p$ is the number of phases and $n$ is the number of the intensive variables necessary to describe the system, except for the mole fractions of the components in each phase. The number of thermodynamic parameters must be specified in order to define the system and all of its associated properties. In electrochemical studies, the intensive variables are only temperature and pressure. Hence, Gibbs' phase rule has the simplified form

$$f = c - p + 2. \tag{3}$$

The cathode can be treated as a binary system ($c = 2$) consisting of Li and $FePO_4$. Since the temperature and the pressure are kept constant in the experiments, the degrees of freedom reduce to

$$f = (2 - p + 2) - 2 = 2 - p. \tag{4}$$

If only one phase exists in a particle, $p = 1$ and $f = 1$; therefore, the potential has a degree of freedom and varies with the lithium concentration. On the other hand, if the particles contain two phases (Fig. 1a), $p = 2$ so that $f = 0$, in which case no intensive variable has a degree of freedom, *e.g.* the cell potential cannot change (Fig. 1b); it is a constant, $V_0$.

$$V(x) = V_0 \tag{5}$$

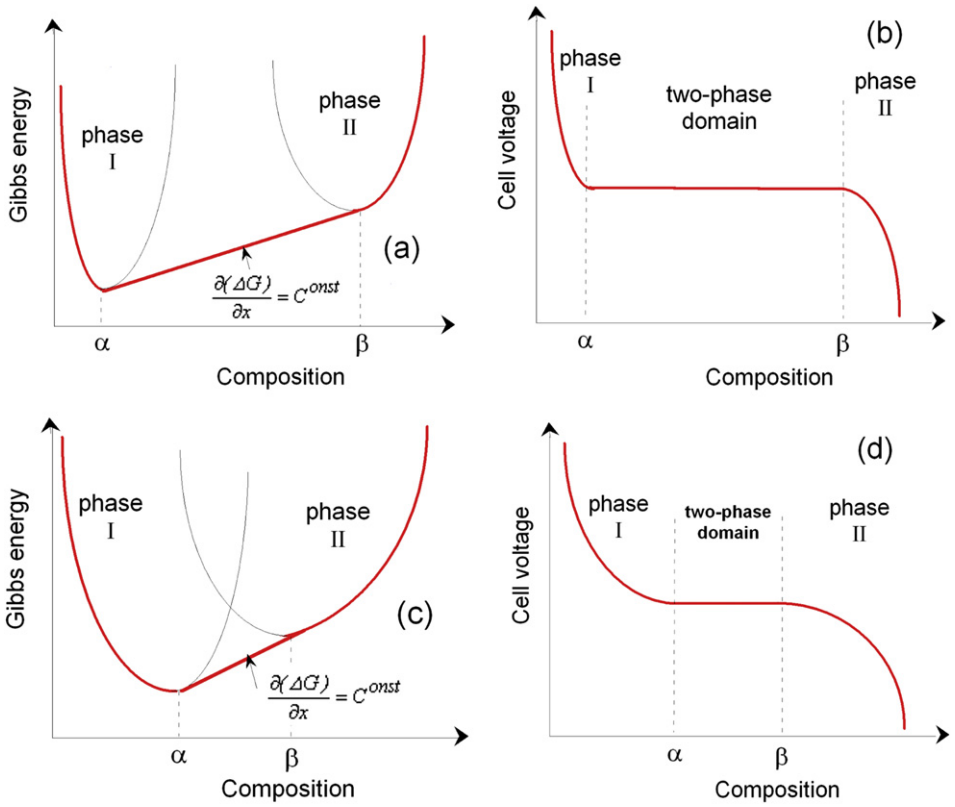


**Fig. 1.** Schematic representation of the Gibbs rule for a two-phase system and cell voltage *vs.* composition for bulk material (a,b) and nanosized material (c,d). A voltage plateau appears between the instabilities between phases.

and $\Delta G$ is linear in $x$ according to Eq. (1). A general feature is the fact that the insertion or de-insertion process for the $Li_xMPO_4$ bulk material is a two-phase process. It means that the $Li_xFePO_4$ solid solution does not exist unless $x$ is close to zero or close to 1. As a consequence, a rapid de-mixing occurs, and we are left with two phases, namely $Li_{1-\alpha}FePO_4$ (Li-rich) and $Li_\beta FePO_4$ (Li-poor), where $\alpha$ and $\beta$ denote the width of the single-phase regions in Fig. 1 [18]. For big particles, $\alpha \approx \beta \approx 0$, and we can simply write the bulk material at intermediate concentrations under the form $xLiFePO_4 + (1 - x)FePO_4$. For nanoparticles, the two-phase domain is reported to shrink [18] (Fig. 1c), and the voltage plateau is shorter (Fig. 1d).

## 3. Ionic conduction

The orthorhombic structure of the ordered olivines $LiMPO_4$ (Fig. 2) contains a framework of $PO_4$ complexes strongly bonding in the three dimensions (3D) layers of $M$ cations in octahedral coordination. The strong 3D bonding of the olivine framework, which contrasts with only 2D strong bonding in the layered cathodes, *e.g.* $LiCoO_2$, is responsible for their strong thermal stability. Theoretical [20,21] and experimental [18] studies have shown that the guest $Li^+$ moves in this framework along [010] channels in the open space between the $PO_4$ units. The motion is not a straight line. Instead, the $Li^+$ ions can be viewed as slalom racers inside their channel; but the trajectory is 1D. The drawback of this property is that the ionic conductivity is extremely sensitive to any defect or impurity that is able to block a channel, thus preventing the diffusion of the $Li^+$ ions to all the sites in a channel. This problem has been an obstacle for years for the industrial development of the material for Li-ion batteries; but fortunately the problem has been solved, and it is now possible to prepare the material free of impurities. Another particularity is the fact that segregation of the two phases, Li-poor and Li-rich, say $FePO_4$ and $LiFePO_4$ to simplify, originates in Coulomb correlations [22] that have observed experimentally with transmission electron microscopy [23–26]. The symmetry of the lattice and the preferential diffusion of Li along the $b$-direction are not sufficient to determine the geometry of the $FePO_4/LiFePO_4$ interface, which can lie in the ($bc$) plane [23] or in the ($ac$) plane

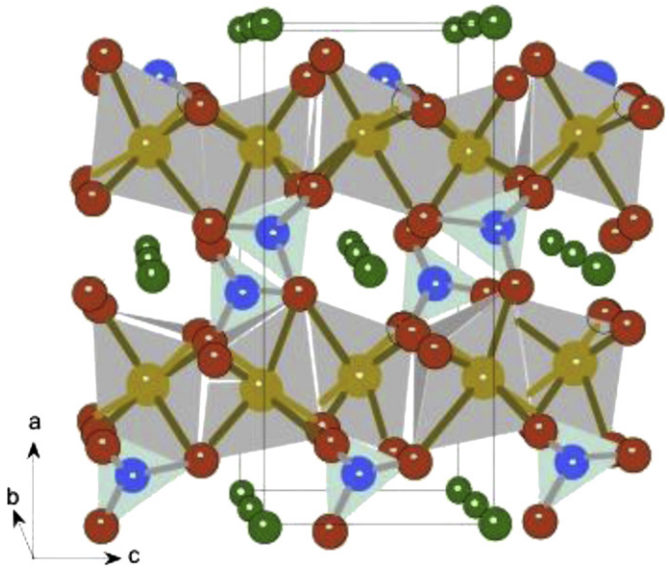


**Fig. 2.** Scheme of the olivine structure of $LiMPO_4$ ($M$ = Fe, Mn, Ni, Co). Li in green, $M$ in brown, P in blue, O in red (For interpretation of the references to color in this figure legend, the reader is referred to the web version of this article.).

[25]. The Li*M*$PO_4$ olivine nanoparticles crystallize in platelets with the [010] direction perpendicular to a (*bc*) platelet in $LiFePO_4$, but lying within an (*ac*) platelet in $LiMnPO_4$ [27,28] and $LiCoPO_4$ [29]. Consequently, the Li diffusion length is short and parallel to the two-phase $FePO_4$/$LiFePO_4$ interface whereas in $LiMnPO_4$ and in $LiCoPO_4$ the Li diffusion length is larger and its path is intersected by the two-phase interface [27]. The formation of $FePO_4$ domains upon Li extraction has clearly been observed [23]. The mosaic model [26] takes into account the possibility that the extraction/insertion of lithium starts at different nucleation sites. An open question is whether these nucleation sites are located at several points on the crystal surface [23] or are more distributed below the surface. In addition, the topology of the domains depends not only on the models, but also on the sample: in some cases, we have images of stripes [23], or shells [25]. In any case, like in any self-organized system, there is a characteristic length of the pattern formed by the $LiFePO_4$ and the $FePO_4$ domains. In any spinodal decomposition of a 3D material where the interface is not flat, this modulation parameter $\lambda_c$ is simply the typical width of wrinkles that form a labyrinthine pattern [30]. In the present case, however, where the interfaces remain flat, the structure takes the form of periodic stripes in the (*bc*) plane with a lamellar spacing $\lambda_c \approx 50$ nm well observed [23]. In some case, defects prevent the formation of stripes and $\lambda_c$ is the size of finite domains; indeed, the same value $\lambda_c \approx 50$ nm has been observed in that case [30].

This situation should then prevail until the diameter $d$ of the particle is reduced below the order of $\lambda_c$. It implies that there should be an interface between Li-rich and Li-poor phases in a particle partly delithiated provided that $d \geq 50$ nm. This has been contested in a work [31] reporting that the image of an assembly of particles of average size $d = 100$ nm showed only particles either Li-rich or Li-poor, *i.e.* $LiFePO_4$ and $FePO_4$ particles if we neglect the small values of both $\alpha$ and $\beta$ of Fig. 1. However, experiments performed on other particles of this size did show the formation of the interface and domains of size $\lambda_c$ [30]. Nazar *et al.* [32] found an explanation of the result in Ref. [31] that takes its origin in the dependence of the thermodynamic properties on the size of the particles [33,34]. Since the partially delithiated particles are two-phase systems, even at the small size used in the experiments [30], the voltage of the $LiFePO_4$ cells is a constant as a function of rate of delithiation $x$ according to the Gibbs law of thermodynamics. Indeed, the voltage profile as a function of the capacity delivered by the cells (or the variation in Li concentration) shows a broad plateau at the redox potential of *ca.* 3.4 V *vs.* $Li^+$/Li. However, to understand the size effects, we need to be much more accurate. At equilibrium, the experimental value of the open-circuit voltage of bulk $LiFePO_4$ is 3.420 V, while that of nanoparticles is 3.428 V [32]. This 8 mV difference is in agreement with predictions by Jamnik and Maier based on the dependence of the chemical potential on the size of the particles [35] and confirms a result found a few years before [36]. This difference, although small, is significant, because it is a driving force that induces an exchange of lithium between two particles of different sizes via the electrolyte that allows for an ionic conductivity. Therefore, in the case of an electrochemical system with a heterogeneous particle size distribution (under low-intermediate current density), the smaller particles will be lithiated first and the larger particles will be delithiated first during charge and discharge in the region of $\alpha < x < 1 - \beta$ for Li*M*$PO_4$. This is indeed what has been observed with $M$ = Fe and Mn [32]. Therefore, the observation of Li-rich and Li-poor particles at intermediate steps of lithiation/delithiation is not evidence that the diffusion of particles of small (say $d = 100$ nm or less) is so fast that Li-poor particles become Li-rich quasi instantaneously and vice-versa as has been claimed [31,37]. Actually, an electrochemical cell with a heterogeneous particle size distribution initially contains two phases inside each particle a short time after use. It is only after the cell has been placed in open circuit mode for a long time (72 h in the experience in Ref. [32]) that electrochemical equilibrium between particles reached, and then the poly-disperse powder contains only single phase particles either Li-rich or Li-poor, depending on their size.

An important literature has been devoted to the Li-diffusion coefficient. Most of the works, however, determine the chemical diffusion coefficient $D_{Li}$ that can be derived from the Fick's law and the Nernst–Einstein equation, which is valid only in the case of solid solutions and uncorrelated motions of $Li^+$ ions. In the present case, this condition is restricted to a small range of concentrations $x<\beta$ or $x > 1 - \alpha$. In between, *i.e.* in the range $\beta<x < 1 - \alpha$, the system is a two-phase system, at least if the size of the particles is larger than 50 nm [32] (we shall discuss smaller sizes later), in which case the diffusion is a coherent motion of $Li^+$ ions responsible for the shift of the interface between the two phases so that the kinetics is rather associated to the motion of this front. Indeed, the diffusion of Li is very anisotropic, large along the *b*-axis and orders of magnitude smaller in other directions [38]. Therefore, the delithiation/insertion of $LiFePO_4$ proceeds by emptying/filling channel by channel with lithium, which is the process by which the interface between Li-rich and Li-poor domains moves. A recent work, however, takes this two-phase process into consideration [39]. The value of the diffusion coefficient according to this model varies within a broad range $10^{-10}$ to $10^{-16}$ $cm^2\ s^{-1}$ depending on the lithium content in solid solution or the $LiFePO_4$/$FePO_4$ phase ratio. The results of galvanostatic and potentiostatic intermittent titration techniques also reported in this work are in good agreement with this model.

Conversely, the above discussion does not mean that the reduction in size of the particles has no impact on the diffusion coefficient. It does have an impact, as smaller particles show better ionic diffusivity for trivial reasons. First, bigger particles are formed of several nanocrystallites oriented randomly and separated from each other by grain boundaries that block the channels [40]. Second, nanoparticles are usually crystallites, so that the channels are open to the surface of the particles through which the $Li^+$ ions can travel fast in $LiFePO_4$ [27,28]. Third, big (say micron-sized) particles, even if they were single crystals, would show small ionic conductivity because the $Li^+$ ions will almost certainly meet an antisite defect (*M* on Li sites) on their long path along their channels before reaching the interior or surface of the particle. This defect, which has a low energy of formation [19,41] has indeed been often observed [42] in these materials, and its dramatic effect on the electrochemical properties has been evidenced [42]. These are the reasons why the effective diffusion in nanosized particles is trivially faster than in big particles. Note also that this discussion implies that the diffusivity of the lithium will not only depend on the size of the particles, but also on their shape, which was the motivation to monitor these two parameters by appropriate synthesis processes reviewed in Refs. [16,17]. Note that this discussion on the reasons for the better diffusivity of nanoparticles with respect to that of the bigger ones takes into account the 1D nature of the ionic conductivity.

## 4. Electrochemical behavior

To investigate the exact role played by the features described in the previous section, let us compare the electrochemical properties of $LiFePO_4$ with those of $Li_4Ti_5O_{12}$. The latter is of great interest since it can be used as an anode material coupled to $LiFePO_4$ as the cathode to build a Li-ion cell that has a very long cycling life (no aging over the 30,000 cycles tested) and great power since the tests have been performed at 10C rate (a charge at *n*C rate means a full

charge in a time $1/n$ hours) [43]. $Li_4Ti_5O_{12}$ crystallizes in the spinel structure with a framework strongly bonded in 3D, with an ionic conductivity that is also three-dimensional. The intercalation of Li is a two-phase process, as in the olivine materials, since it is a two-phase reaction from $Li_4Ti_5O_{12}$ to $Li_7Ti_5O_{12}$. To make comparison, we have prepared two half-cells: C-$Li_4Ti_5O_{12}$//Li and C-$LiFePO_4$//Li. The notations are conventional. The 'C-' symbol to the left means that both the $Li_4Ti_5O_{12}$ and $LiFePO_4$ particles were covered by a carbon film according to the same process [44] to increase the electronic conductivity. In addition, we have chosen particles of $Li_4Ti_5O_{12}$ and $LiFePO_4$ of the same size ($d$ = 90 nm). The counter-electrode is Li metal in both cases, and the electrolyte is also the same ($LiPF_6$ in 1 mol $L^{-1}$ EC + DEC). In summary, the construction of the cells is the same, so that direct comparison is possible. At low C-rates, the charge/discharge flat plateaus are well observed at the redox potentials 3.4 V and 1.55 V for the $LiFePO_4$ and $Li_4Ti_5O_{12}$, respectively, as expected from the Gibbs law for a two-phase conversion process. The performance as a function of the C-rate is reported in Fig. 3 under the form of the modified Peukert plots reporting the dependence of the capacity as a function of the C-rate for the two cells. These plots show that the capacity of $Li_4Ti_5O_{12}$ is about 163 mA h $g^{-1}$, up to 3C rate, only slightly larger than the capacity of $LiFePO_4$ at low C-rate. In addition, the electronic conductivity inside $Li_4Ti_5O_{12}$ is about $10^{-13}$ S $cm^{-1}$ [45], while it is about $10^{-9}$ S $cm^{-1}$ inside $LiFePO_4$ [46]. Therefore, if the power was limited by the electron mobility, one should expect the capacity of the $LiFePO_4$//Li cell to be higher than that of the $Li_4Ti_5O_{12}$//Li at high C-rate. However, just the opposite is observed in Fig. 3. When the C-rate increases, the capacity is decreasing much faster with $LiFePO_4$ than in the case of $Li_4Ti_5O_{12}$. Therefore, the electrons do not limit the charge transfer. This drop of capacity is thus attributable to the increase of the internal resistance at high C-rate where thermodynamic equilibrium cannot be reached in $LiFePO_4$ at a C-rate where the $Li^+$ ions still have time to penetrate into or from the spinel. Therefore, the performance and motion of the Li ions in a $LiFePO_4$//$Li_4Ti_5O_{12}$ cell built with these particles is limited by the diffusion coefficient of the lithium in the olivine framework, not by that in the spinel. Therefore, the 1D nature of the Li transport in $LiFePO_4$ does not seem to be critical to explain the excellent performance of this material at high C-rates, contrary to prior claims by different authors. However, the fact that the Li transfer proceeds through a two-phase reaction is critical because it implies that the nucleation rate is faster than the solid-state diffusion in a particle. Therefore, the outstanding performance at high C-rate obtained with nanosized particles is attributable to the fact that the Li transfer is a two-phase process. The fact that both the olivine and the spinel electrodes have this property is probably a key issue to explain the unequal performance of the $LiFePO_4$//$Li_4Ti_5O_{12}$ cells in terms of power density. In addition, the absence of a solid-electrolyte interface (SEI) layer on $Li_4Ti_5O_{12}$ and the fact that the insertion/deinsertion of Li occurs without change of volume contribute to the performance of the spinel electrode. Such a cell with nanosized particles for both electrodes is operating safely with very long cycling life (thousands of cycles) up to 40C rate as is shown in Fig. 4 [47].

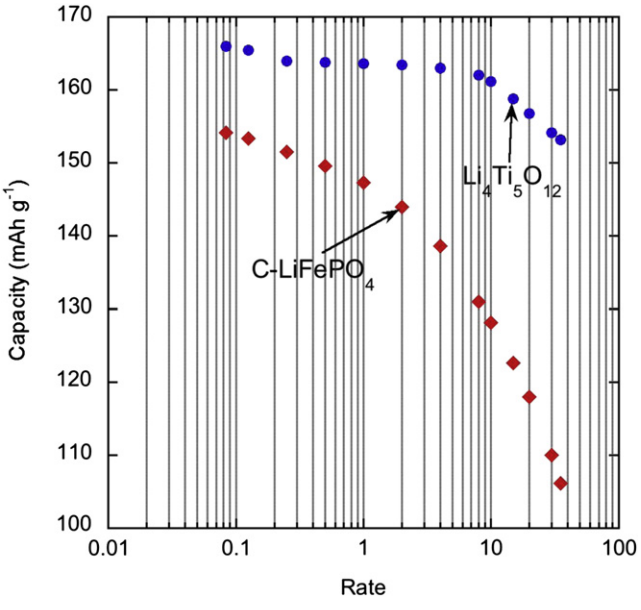


**Fig. 3.** Modified Peukert plot of C-$LiFePO_4$ and C-$Li_4Ti_5O_{12}$ *vs.* $Li^+$/Li. The two powders had the same size (90 nm). The electrolyte was 1 mol $L^{-1}$ $LiPF_6$ in ethylene carbonate (EC) and diethylene carbonate (DEC).

## 5. The surface layer

The surface layer of bare olivine compounds is not entirely amorphous, but it is at least severely disordered over a thickness of 3 nm [48]. This disorder has been repeatedly observed by TEM, and is illustrated in Fig. 5 for $LiFePO_4$ particles. In this particular case, the particles were 40 nm in size. The thickness of this surface layer does depend on the size $d$ of the particles, at least down to $d$ = 40 nm. On the other hand, its effect on the physical and chemical properties depends very much on the particle size, simply because a bigger fraction of the volume of the particle is involved in the surface layer as $d$ decreases. The fact that the surface layer is not

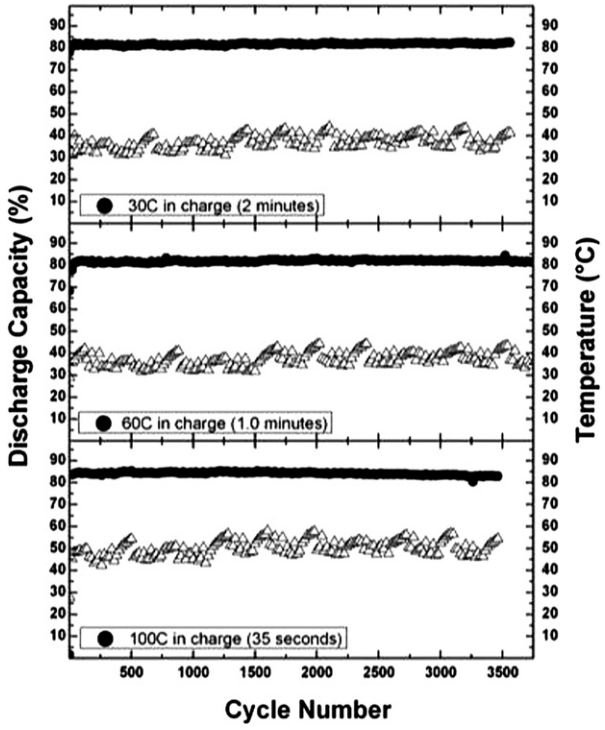


**Fig. 4.** Stability of the "18650" C-$LiFePO_4$/$LiPF_6$ + EC + DEC/C-$Li_4Ti_5O_{12}$ cell built with the same powders as in Fig. 3. Each cycle consists of float charging at 2.5 V during 5 min followed by a discharge at 5C rate. The results are reported as a function of the C-rate of the discharge performed at the beginning of the float. As a result, the cell remains stable over the 3500 cycles that have been tested. The temperature reached by the cell during these experiments (right scale) has been measured with a Fluke Corp. camera, model Ti55, equipped with a lens of 20 mm focal length and aperture of $f$/0.8, operating in the wavelength range 8–14 μm.

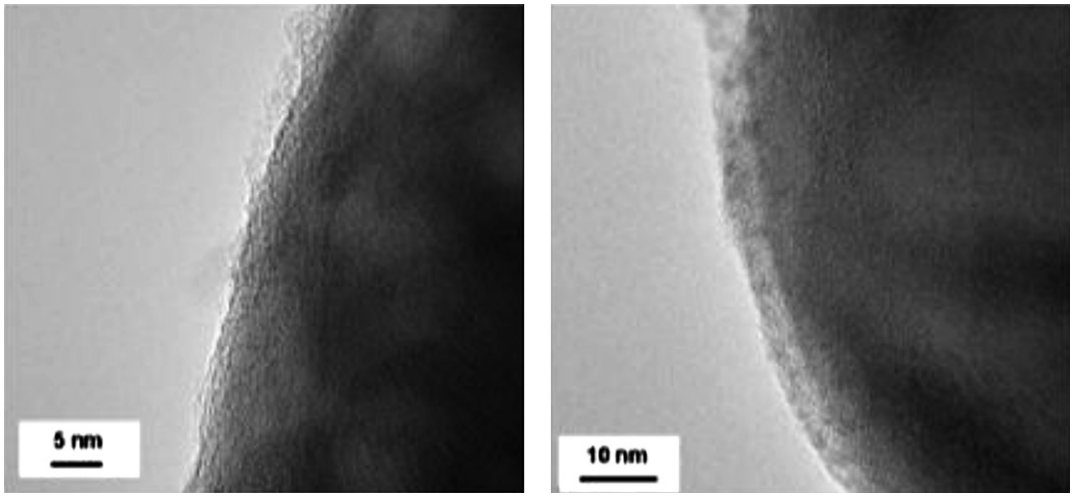


**Fig. 5.** TEM images of the surface of $LiFePO_4$ particles before carbon coating (left) and after carbon coating (right). Note the granular aspect of surface before carbon coating. The lighter part surrounding the particle on the right side is the carbon layer, deposited on a surface that is less disordered.

well crystallized implies that its structural, and thus its physical and chemical properties, are different from the bulk. As an extreme case, the simple extrapolation to small sizes suggests that a particle of size 6 nm (twice the thickness of the disordered surface layer) would be amorphous. We are not aware of any investigation on such small particles; but indeed, there are some trends toward more structural disorder upon decreasing the size to the nano-range. It has been proposed that particles smaller than $d = 70$ nm are amorphous, except if the overpotential (defined in the model as the magnitude by which the potential exceeds the material's equilibrium Nernst potential) exceeds 70 mV [49,50]. In the same spirit, several works report that such small particles are crystallites originally, but become amorphous upon cycling [51]. Nevertheless, we have found that particles as small as $35 \pm 5$ nm remain crystallized [52] even after 30,000 cycles performed at 10C rate [43].

If the material is amorphous, the structural disorder at the molecular scale is expected to destroy the coherent motion of the lithium since the notion of a 1D Li channel is lost. Therefore, amorphization is expected to stabilize a homogeneous $Li_{1-x}Fe_xPO_4$ solid solution. In such a case, the plateau voltage *vs.* $x$ at 3.4 V $Li^+/Li$, characteristic of the two-phase system, should be replaced by a continuous variation of the voltage as a function of $x$. Indeed, experiments reported in the literature show that the plateau shrinks with the particle size, which has been interpreted [36,53] as a sign that the miscibility gap decreases with $d$. According to Ref. [53], the end-members for the two-phase process in nanoparticles are given by $\alpha \leq 0.89$ and $\beta \geq 0.05$. Gibot *et al.* [54] even reported that the voltage plateau is no longer observed in particles with $d = 40$ nm. In this last case, however, the particles were ill crystallized with many defects so that, in our view, the result should rather be interpreted as confirmation that structural disorder, rather than a size effect, favors a solid solution instead of a two-phase configuration. Indeed, the electrochemical measurements performed on crystallites of the same size and free of defects show the plateau [48], as can be seen in Fig. 6. One other effect might also make questionable the interpretation of the shrinking of the plateau. One of them comes from the fact that the powders used to build the cathode are never mono-dispersed. We have already pointed out in this review that a consequence of the heterogeneity is that particles are either in the $Li_{1-\alpha}FePO_4$ (Li-rich) or in the $Li_{\beta}FePO_4$ (Li-poor) phase if they are left at open-circuit voltage for a time long enough so that electrochemical equilibrium between the particles can be reached by exchange of $Li^+$ ions via the

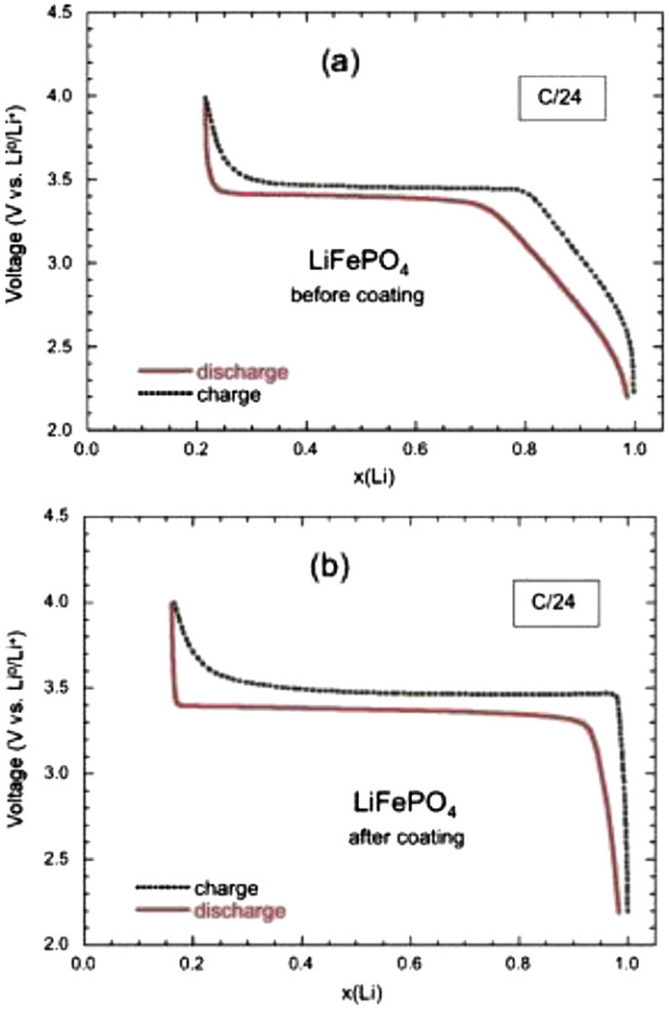


**Fig. 6.** Charge/discharge voltage profiles of $LiFePO_4/LiPF_6$–EC–DEC/Li cells with the cathode prepared with the 40 nm sized $LiFePO_4$ particles before carbon coating (a) and after carbon-coating (b), from Ref. [44].

electrolyte. In such a situation, crystallites having a wide particle size distribution would display a sloping $V(t)$ profile similar to a solid-solution behavior, as noted in Ref. [32]. Moreover, 11% of the volume of a particle of size 40 nm is in the disordered surface layer 3 nm thick [54]. We thus expect the solid solution to be stabilized in this part of the particle, while the kinetics inside the core region would impose still a two-phase process. Such a situation will also alter the voltage plateau, the shrinking of which would reflect this disordered structure in the particles (Fig. 5a), when the surface layer has not been modified by a surface coating (Fig. 5b). Therefore, both the propagation of the disorder from the surface layer to the core region of the particles upon decreasing the size of the particles and the increase of the disorder toward amorphous state are still open questions that may not occur at size $d > 35$ nm. An increase of the disorder and the related stabilization of the solid solution upon lithiation/delithiation as a result of configurational entropy is expected, but only for systems with a number of Li atoms of the order of $10^3$, corresponding to systems smaller than 4 nm [55]. This limit is also the typical size predicted by calculation of the electronic structure, including surface energy aspects [56]. Finally, we have already noticed that we could synthesize particles of size 35 nm that were well crystallized and kept a voltage plateau characteristic of a two-phase process. On the other hand, we have also noted that the characteristic length of the self-organized two-phase regime was in the order of 50 nm. Significantly, therefore, smaller sized particles might prefer a solid solution because of the energy of the diffuse interface between the Li-rich and Li-poor phases as has been predicted by some [57,58] for particles of size $d < 35$ nm.

Since the discussion in the previous section led us to conclude that the two-phase kinetics was a key parameter to explain the electrochemical performance, the present discussion suggests that the optimum size of the $LiFePO_4$ particles should be about 35 nm, as the reduction of the size below this value would lead to a tendency toward more structural disorder. This conclusion is consistent with the fact that the performance in terms of power density of a $LiFePO_4$-based battery is actually increased upon decreasing the size of the particles down to 35 nm [54].

## 6. Surface modification

The capacity retention of a cathode active material is strongly dependent on the surface chemistry of the host particles, which are always covered by surface films limiting the Li-ion migration and their charge transfer across the active interface [59]. That is true for any cathode element, and $LiFePO_4$ is no exception. But in addition, the $MPO_4$ hosts have a poor electronic conductivity, which is why the $LiFePO_4$ particles must be coated with a layer of conductive carbon, following the pioneering work in Ref. [15], before they can be used as cathode elements in batteries. The carbon coating is a good example of serendipity, and it took time to understand the reasons for the huge improvement of the electrochemical properties observed upon carbon coating. It was immediately attributed to the improvement of the electronic conductivity, the carbon transporting electrons between the current collector and the particle surface. This explanation, however, is only a part of the answer. Carbon coating also helps in removing the impurities that can poison the material [60]. The first hypothesis that has been invoked to explain this effect is a carbothermal effect. Indeed, the carbon is a reducing agent that might avoid the formation of $Fe^{3+}$ impurities, but only at much higher temperatures than the temperature available in the carbon coating process, which must be limited to 700 °C to avoid the degradation of the $LiFePO_4$. The reduction power comes from the fact that the precursor of the carbon is and must be a polymer, *i.e.* a material that contains hydrogen, and the hydrogen is the reducing agent [61]. So the removal of the impurities is actually an important side effect of the carbon coating itself. But this deduction is still not sufficient to explain the outstanding performance of the carbon coating process. Usually, the carbon deposited at low temperature is not conductive because it includes many $sp^3$ bonds. To have a conductive carbon layer deposited on silicon, for instance, one needs to make the deposit at *ca.* 900 °C. However, on $LiFePO_4$, the temperature 650 °C is sufficient to obtain a conductive carbon layer [62–64]. There is thus a catalytic effect associated to the Fe–C interactions (also known to play an important role in biology). Moreover, we have noticed that, after the carbon coating, the disordered surface layer of $LiFePO_4$ has been crystallized [44]. We have shown that this is an annealing effect of the heating process at 650–700 °C that heats the surface reconstruction at the particle surface during the carbon coating process: another beneficial side effect. The combination of these effects of the carbon coating process implies that a reductive coating of $LiFePO_4$ is mandatory. All these effects are observed for particles of any size, at least in the range $d \geq 35$ nm where it has been tested: after the coating, the $LiFePO_4$ particles are well-crystallized, free of impurities, the disorder of the surface layer has disappeared, and the particles are covered with a 3-nm-thick layer of conductive carbon. This situation is illustrated in Fig. 5b. Note that the benefit in the case of nanoparticles is much more important than in the case of bigger particles: a disordered surface layer that is 3-nm thick involves a negligible part of a micron-sized particle, but it is an important part of a particle of size $d = 35$ nm and plays a role in the discussion of the size effect reported above. We have already mentioned the role of the impurities and amorphization to stabilize a solid solution rather than the two-phase lithiation/delithiation process. The reduction in size of bare particles undoubtedly increases the overall structural disorder and favors amorphization simply because the thickness of the surface layer is independent of $d$. For C-$LiFePO_4$, *i.e.* carbon-coated particles, however, the reduction in size is not affected by a disordered surface layer, at least when the size is not decreased below 35 nm, since the disordered layer has been re-crystallized as can be seen in the TEM image in Fig. 5b. Moreover, the plateau characteristic of the two-phase region is recovered after carbon-coating as can be seen in Fig. 6 for particles of size $d = 40$ nm, which shows that the two-phase insertion/deinsertion process is recovered even for such small particles.

## 7. From multi-ion to multi-composite nanoparticles

$LiMnPO_4$ is even more insulating than $LiFePO_4$ [65]. Therefore, the only hope to make it competitive as a cathode element is to follow the same guidelines that proved successful for $LiFePO_4$, *i.e.* decrease of the size to the nano-scale and coat the particles with conductive carbon. Indeed, $LiMnPO_4$ particles of size ~50 nm have been obtained by different synthesis routes: solid-state reaction in molten hydrocarbon [66], polyol synthesis [67,68], spray pyrolysis plus ball milling [69]. The best result has been obtained by Choi *et al.* who synthesized $LiMnPO_4$ nanoplates with a thickness of 50 nm that are assembled and grew into nanorods along the [010] direction in the (100) plane [66]. The capacity 168 mA h $g^{-1}$ at very low rate C/50 obtained in this case is close to the theoretical value. At faster rates, however, crucial for electric vehicles that require high power supplies, $LiMnPO_4$ still cannot compete with $LiFePO_4$ because of the orientation of the two-phase interface relative to the [010] diffusion path [27]. Now comes the hard part, the coating, and we have already shown in the previous section that this step is mandatory. The problem is that the catalytic effect of Fe that was so useful in the case of $LiFePO_4$ is lost in the case of Mn so that the coating is much more difficult. Indeed, despite many efforts made

to obtain C-$LiMnPO_4$ [70–75], the capacity remains smaller than that of $LiFePO_4$. The low reactivity of $LiMnPO_4$ with carbon may explain that capacities of 130–140 mA h $g^{-1}$ at rate C/10 can be obtained only if the particles are immersed in a huge quantity of carbon, typically 20 wt.% [76] up to 30 wt.% [69,77], while it cannot exceed a few wt.% in commercial batteries. Another reason for the relative inefficiency of the carbon coating of $LiMnPO_4$ comes from the rapid degradation of the material and a heterogeneous carbon layer upon calcination at temperature $T_{ca} \geq 650$ °C [78]. However, this is the minimum temperature that is needed to insure that the carbon layer is conductive in the case of $LiFePO_4$, and we have already pointed out that $LiFePO_4$ is a very favorable case, since higher temperatures are usually required. This limitation in $T_{ca}$ implies that the carbon deposit on $LiMnPO_4$ probably does not have a good electronic conductivity. These different elements explain that the performance of $LiMnPO_4$ as a cathode element is below that of $LiFePO_4$: the current durability in $Li_xMnPO_4$ is orders of magnitude smaller than that of $Li_xFePO_4$ [79,80], and kinetics is slower [81,82].

The first idea to overcome this difficulty was to investigate the $LiFe_yMn_{1-y}PO_4$ solid solution that exists at any composition $y$ to find a compromise, namely a composition $y$ large enough to keep the benefit of the carbon coat due to the iron, but small enough to take the maximum benefit of the higher working potential with Mn [83]. The result is that the optimum value of $y$ is in the range $0.5 \leq y < 0.8$ [84,85] in which a capacity retention *ca.* 120 mA h $g^{-1}$ has been obtained at rate 1C.

An improvement has been obtained recently, owing to a multi-composite synthesis process in three steps, detailed in Ref. [86], that can be briefly summarized as follows. First step, the $LiMnPO_4$ particles were synthesized. Second step, a solution that contains the precursors of $LiFePO_4$ is added to the $LiMnPO_4$ particles and the mixed system is heated. As a result, the $LiMnPO_4$ particles are coated with a thin layer of $LiFePO_4$ in a synthesis process at low temperature (220 C for these two steps). Third step, these composite particles are coated with carbon by following the lactose route involving a heating limited to 600 C during 7 h to avoid the degradation of $LiMnPO_4$ at higher temperature. The TEM image [86] showing the different layers of the multi-composite particles is shown in Fig. 7. The interface between $LiMnPO_4$ and $LiFePO_4$ is sharp. The thickness of the $LiFePO_4$ layer varies from 10 to a few tens of nanometers. The thickness of the carbon layer on top is still about 3–5 nm-thick as in C-$LiFePO_4$. Compared with Fig. 5b, however, the interface between $LiFePO_4$ and the carbon layer is less regular, simply because the calcination temperature at 600 °C is about 50 °C smaller than the optimum temperature needed to obtain the sharp interface of Fig. 5b. The time 7 h spent at 600 °C is needed because the *in-situ* TEM observations [44] show that the dynamics of the re-crystallization of the surface layer at 600 °C is rather slow. Indeed, we can see in Fig. 7 that the $LiFePO_4$ layer, although it is thin, is well crystallized. The composite particles are made of 2/3 $LiMnPO_4$ core for 1/3 $LiFePO_4$ coating layer. It is then of interest to compare the electrochemical properties of these particles with those of a powder of $LiMn_{2/3}Fe_{1/3}PO_4$ particles, which have the same proportion of Fe and Mn and the same size, inasmuch as this composition corresponds to $y = 0.66$, in the optimum range we have defined earlier as $0.5 \leq y < 0.8$. The result is illustrated in Fig. 8, showing that the capacity of the multi-composite particles has been improved by a factor 2–3, depending on the C-rate. Moreover, the cyclability is very good over the 100 cycles where the tests were made. The multi-composites were not yet nanoparticles, since their size was ~300 nm. Also a recent work suggests that the temperature can be raised to 650 °C without damaging $LiMnPO_4$ [78]. The next step will thus be to optimize the synthesis conditions in order to decrease the size of the $LiMnPO_4$ core down to the nano-range, and increase by few tens of degrees the temperature of the carbon coating, since those are the two key parameters. Already the results on the multi-composite particles in which only the $LiFePO_4$ and the carbon coat were "nano" are very promising.

Of course, if the $LiFePO_4$-coating of $LiMnPO_4$ has been successful, it will be *a fortiori* for $LiFePO_4$-coating of $LiMn_yFe_{1-y}PO_4$ for any composition $y$ of the solid solution, and actually, the recipe has already been used for $y = 0.88$, with results similar to the expectation [87]. This composition, however, should not be the best, since the best electrochemical performance on these alloys have been obtained for $y < 0.8$. The whole series $LiFePO_4$-coated $LiMn_yFe_{1-y}PO_4$ has yet to be explored in the range of compositions $0.5 < y < 0.8$ that is the most promising.

The fact that the multi-composite C-$LiFePO_4$//$LiMnPO_4$ has better electrochemical properties than the multi-ionic $LiMn_yFe_{1-y}PO_4$ with the same proportion of [Mn]/[Fe] at any rate was not necessarily expected. We can, however understand this result if we

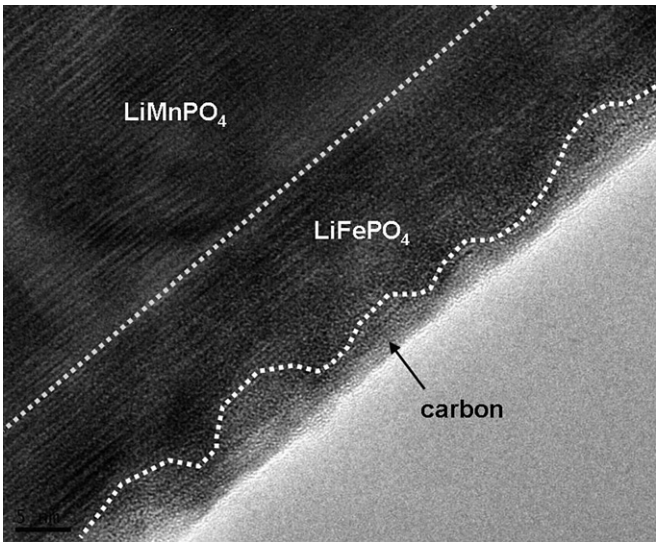


**Fig. 7.** TEM image near the surface of a particle of the composite showing the different layers. Note the interface between $LiMnPO_4$ and $LiFePO_4$ is sharp. The carbon layer is continuous, but irregular, as a consequence of the rather low calcination temperature 600 °C.

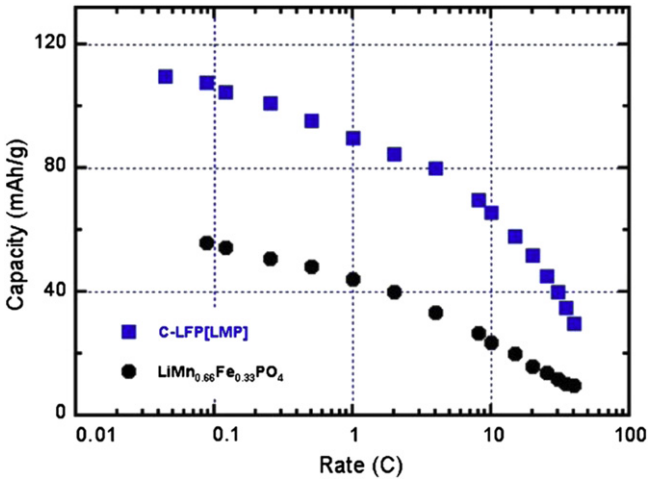


**Fig. 8.** Modified Peukert plot of the C-$LiFePO_4$–$LiMnPO_4$ and $LiMn_{2/3}Fe_{1/3}PO_4$ samples (same overall ratio of Mn over Fe, same size $d = 300$ nm of particles) for comparison.

note that the Jahn–Teller distortion associated to the presence of $Mn^{3+}$ is increased by the alloying effect in the solid solution, because the presence of $Fe^{2+}$ prevents the distortion to propagate at a long range scale. Therefore the lattice as a whole cannot accommodate this distortion that remains localized in the vicinity of the $Mn^{3+}$ ions, which increases significantly the strain field. This important strain field in $LiMn_yFe_{1-y}PO_4$ has been evidenced in Ref. [85]. These important local distortions may reduce the diffusivity of the $Li^+$ electrons, and are presumably the reason for the limited performance of the multi-ionic particles with respect to the multi-component ones. Indeed, the poor performance of cathode elements of binary compounds is not limited to the case of the $LiMn_yFe_{1-y}PO_4$. This may also explain the rather poor performance of $LiMPO_4$ when $M$ is a mixture of Fe with other transition metal ions. This is true for $LiNi_yFe_{1-y}PO_4$ [88], which is not surprising since $Ni^{3+}$ is also a Jahn–Teller ion, but this is also true for $LiCo_yFe_{1-y}PO_4$ [89], presumably due to an instability at the too high voltage. In both cases, the partial substitution of Fe only results in a decrease of the capacity and lower capacity retention. It is then not surprising that the same degradation in the performance is observed in ternary compounds [90–92], or quaternary compounds [93] that mix these Fe, Mn, Ni and Co ions. Indeed, one reason for the remarkable performance of $LiFePO_4$ may also be due to the fact that the $Fe^{2+}$ ion is not a Jahn–Teller ion, and the $Fe^{3+}$ ion in the delithiated material is not a Jahn–Teller ion either because it is in the high spin state.

The cation mixing Fe, Mn, Ni and Co aimed to increase the operating voltage to gain in energy density. However, other cation mixing has been attempted, aiming to some doping in order to increase the electronic conductivity [94]. Such an increase first attributed to supervalent doping [94] turned out to be due to the carbon liberated from the synthesis precursors [46,95] and also metallic iron phosphides/carbophosphides on the $LiFePO_4$ surface arising from solid-state reactivity at the elevated temperatures used in processing [96]. In addition, in such a ionic compound, the limit of solubility of a supervalent ion in substitution is necessarily very small, if not impossible for basic reasons detailed in Ref. [46]. Nevertheless, the insertion of some of supervalent dopants (Zr,Nb,Cr) is possible, but only to the extent of 3 mol%, and in addition, these dopants are located primarily on the Li sites, not to the Fe sites [97], in agreement with predictions [98]; the dopant charge is compensated by Li vacancies. As a result, the dopant on the Li sites block the Li-channels, so that the insertion of these supervalent ions is detrimental to the electrochemical properties, and indeed, none of these doped samples could reach the performance of C-$LiFePO_4$. Note this result has been established in Ref. [97] for bulk samples. Will it be different in nano-sized particles? As we already discussed, nanoparticles with a size the order of 10 nm are expected to be amorphous, which will then stabilize the solid solution $Li_xFePO_4$ instead of the two-phase system along cycling. The doping should not favor crystallization. But while some people still believe that the homogeneous solution would be beneficial to the electrochemical properties, we have given arguments that the opposite should hold true, because the coherent motion of Li that allows for fast lithiation–delithiation process would be lost. In addition, the study of the $LiFePO_4$ particles of any size $d > 35$ nm after delithiation shows that the $Fe^{3+}$ ions that are in high-spin state in the crystallized phase are in the low-spin state in the disordered surface layer, which means that the disorder favors the low-spin state for this ion. But while $Fe^{3+}$ is not a Jahn–Teller ion in the high spin state, it is a Jahn–Teller in the low-spin state. According to the importance of the Jahn–Teller effect outlined in the previous lines of this review, this is clearly another reason why the doping should not improve the electrochemical properties. And indeed, while we have shown in the previous sections that C-$LiFePO_4$ can deliver more than 160 mA h $g^{-1}$ at low C-rate, and can be charged/discharged at 40C rate without aging over 20,000 cycles, no sample with Fe partly substituted by one or more transition element has ever been able to approach this performance. For these different reasons, we believe that the new route to multi-composite systems is much more promising than the multi-ion synthesis.

Another advantage of multi-composites comes from the fact that $LiFePO_4$ can be used to coat other cathode particles that do not belong to the olivine family. Such a coating led to a remarkable improvement of the electrochemical performance of $LiCoO_2$ [99] and $LiNi_{0.5}Co_{0.2}Mn_{0.3}O_2$ [100], as the $LiFePO_4$ coat improves safety and brings protection against reactions with the electrolyte to these lamellar compounds. Another example is the $LiMn_{1.5}Ni_{0.5}O_4$ (LMN) spinel, of great interest because it provides access to the Ni(IV) to Ni(II) formal valences at about 4.7 V *vs.* $Li^+$/Li [101,102]. However, the cathode/electrolyte surface reactions lead to degradation in the electrochemical performance [103]. Surface modifications with nanosized $Al_2O_3$, ZnO, $Bi_2O_3$, and $AlPO_4$ suppress the formation of thick SEI layers on $LiMn_{1.42}Ni_{0.42}Co_{0.16}O_4$ [103], already improving the electrochemical performance. These coats, however, are not active materials. More recently, C-$LiFePO_4$ was coated $LiMn_{1.5}Ni_{0.5}O_4$ (LMN) by a mechano-fusion dry process [104]. After 20 wt.% of coating, the LMN surface was uniformly covered by $LiFePO_4$. The voltage profile for the two first cycles between 3.0 and 4.9 V *vs.* $Li^+$/Li at C/24 rate are reported in Fig. 9 after C-$LiFePO_4$ coating and before, for comparison. The characteristic 3.5 V (couple $Fe^{3+}/Fe^{2+}$) plateau is clearly seen in this figure, in addition to the 4.7 V plateau characteristic of the spinel part. The C-$LiFePO_4$ part is thus active, which is an advantage with respect to the previous coatings [8], and the capacity has been improved. Until 10C-rate, the capacity was found to be the simple addition of the capacities of the C-$LiFePO_4$ and the $LiMn_{1.5}Ni_{0.5}O_4$ at the corresponding rate. On the other hand, at faster rate, the capacity was found to be much larger than the simple addition of the components (see Fig. 10). Therefore, the capacity of $LiMn_{1.5}Ni_{0.5}O_4$ has increased, proof that the C-$LiFePO_4$ has increased the surface conductivity and has protected $LiMn_{1.5}Ni_{0.5}O_4$ against reactions with the electrolyte. We should be aware, however, that the race to higher voltage poses other questions, like the one posed by R. Huggins in the title of an oral communication at the PRIME conference this year: "Do we really want an unsafe battery?" pointing out that "increasing voltage above 3 V will sooner or later lead to a disaster because, at the end, chemical

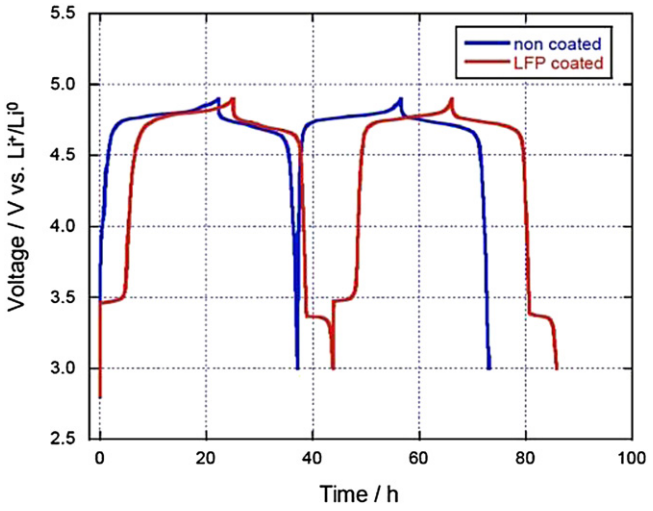


**Fig. 9.** Voltage profiles of the Li//$LiMn_{1.5}Ni_{0.5}O_4$ and Li//C-$LiFePO_4$-coated $LiMn_{1.5}Ni_{0.5}O_4$ cells between 3.0 and 4.9 V *vs.* $Li^+$/Li at C/24 rate. The electrolyte was 1 mol $L^{-1}$ $LiPF_6$ in ethylene carbonate (EC) and diethylene carbonate (DEC).

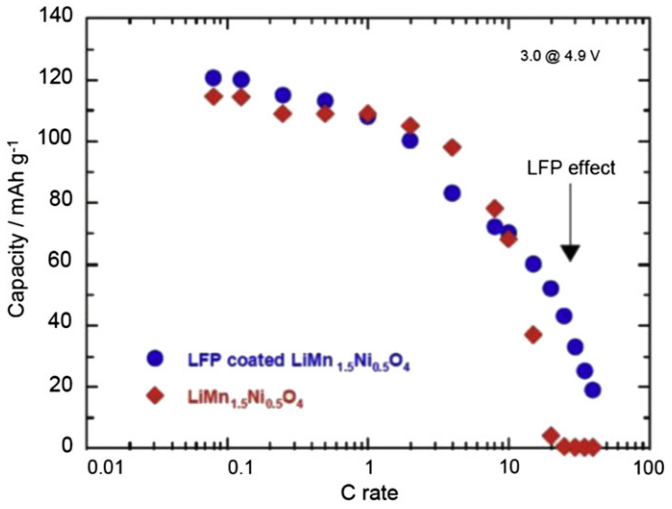


**Fig. 10.** Modified Peukert plot of $LiMn_{1.5}Ni_{0.5}O_4$ C-$LiFePO_4$-coated $LiMn_{1.5}Ni_{0.5}O_4$ measured with the cells as in Fig. 9.

thermodynamics always win" [105]. By this formula, he expressed the concern that the pressure of oxygen at thermodynamic equilibrium in all the oxides of transition metals increase linearly with the potential, favoring the loss of oxygen that causes thermal runaway and battery fires. We shall not discuss here the safety concern, since it is not the purpose of the present paper, which has been reviewed recently elsewhere, but it is something that we should always have in mind when Fe is substituted by another metal just to increase the energy density in any cathode element of a Li-ion battery. Actually, the olivine family may escape to this instability owing to the strong covalent P—O bonding that makes the material a $PO_4$-metal ion compound instead of an oxygen oxide. On another hand, it turns out to be very difficult to obtain $LiMn_{1.5}Ni_{0.5}O_4$ without oxygen vacancies for instance [106], which corroborates the argument of R. Huggins. In addition, formation of the oxygen vacancies in $LiMn_{1.5}Ni_{0.5}O_{4-\delta}$ implies that a fraction of manganese ions switch to the $Mn^{3+}$ valence state to insure local charge neutrality, and we have just shown above how the Jahn–Teller distortion associated with it affects the electrochemical performance. Therefore, the coating of the cathode particles working at 4 and 5-V by $LiFePO_4$ known for its outstanding thermal stability might also prove to be useful to protect the core region against the loss of oxygen, and thus increase the thermal stability at the same time as it increases the electrochemical properties. This may be another reason why multi-component particles may be preferred to multi-ion particles.

The limit in the energy density comes from the fact that only one Li per chemical formula can be extracted from the olivine. Therefore a lot of efforts are currently done do find a new chemistry that would make possible the extraction of two $Li^+$ ions instead of one, in order to replace $LiFePO_4$ in the future by a cathode element that would provide an energy density sufficient to meet the demands necessary to make the electric vehicle fully commercially viable. One solution that is envisioned is the replacement of the phosphorous with silicon. Two materials from a new family of transition metal silicate, namely $Li_2MnSiO_4$ and $Li_2FeSiO_4$ have been successfully prepared and preliminary tested for positive electrode materials. [107–111]. These materials are even more insulating than the LiFe(Mn) olivines, but again, the same solution has been found to overcome the problem, namely carbon coating, not only of the end members, but also of the solid solution $Li_2Fe_{0.5}Mn_{0.5}SiO_4$ [112]. If the two $Li^+$ ions might be extracted reversibly, the theoretical capacity would be raised to about 333 mAh $g^{-1}$. Unfortunately, reversible two-lithium-ion capacity has not been achieved due to the structural instability of these transition metal silicates. This failure can be understood if we remind that the thermal stability of $LiFePO_4$, despite the Huggins argument above mentioned, comes from the formation of the strongly bonded $PO_4$ ion, which is exactly the ion that has been removed to form silicates. The consequence is a structural instability of these transition metal silicates and the subsequent amorphization that has been observed during studies of the charge/discharge operation [113,114], associated to the very large variation of volume in the lithiation and the delithiation processes. To overcome this problem, the only possibility is again to decrease the size of the particles to the nano-range, so that the range of the strain field is larger than the size of the particles, in which case we can hope that the lattice distortion can be accommodated not locally but by the particle as a whole. Indeed, in a recent work [115], Rangappa *et al.* have succeeded in preparing ultrathin nanosheets of $Li_2(Fe,Mn)SiO_4$ that has a capacity close to theoretical with a good capacity retention over 20 cycles. This is a remarkable example of the improvements that the recent nanosheet technology can bring to the field of the Li-ion batteries, since the nanosheets combine two essential properties: large surface area (which is desired to increase the surface contact with the electrolyte), and nanoscopic thickness. Of course, the stability over 20 cycles does not make the material eligible for its use in Li-ion batteries, since reversible two-lithium-ion capacity with stable cyclic performance requires a cathode that is stable toward structural and volume changes during thousands of cycles. Nevertheless, this result is remarkable if we note that it was not possible to make more than one or two cycles before. It is then a motivation to pursue the research in this field, and it illustrates that the nano-science and technology raise the hope for the increase in the energy density of Li-ion batteries in the future.

Another new route to achieve a breakthrough in the performance of batteries is to think of a post-lithium technology. A lot of efforts in research are currently done on Na-batteries, since the sodium is not expensive and widely distributed in the nature, but this is out of the scope of the present review that is focused on olivines. In this context, Mg-batteries have been suggested as a solution, as the insertion/removal of divalent Mg, if successful, results in a nearly doubled cathode capacity compared with Li ion batteries using the same $Li(FeMn)PO_4$ cathode, as the lithium is monovalent [116]. In this theoretical study, however, the authors find that the best potential of using the olivine compounds as Mg battery compounds is $Mg_{0.5}FePO_4/FePO_4$ was suggested to have the potential to insert half Mg with a suitable voltage within the electrochemical window of the electrolytes at the current stage. However, the interest in Mg-batteries rather than Li-batteries relies on the possibility to have one Mg substituted for one Li, and if 2Li are replaced by one Mg, then the advantage is entirely lost, so that this route to increase the energy density does not seem justified so far.

## 8. Conclusions

First, $LiFePO_4$ Li-ion batteries or nano lithium-ion batteries as they are sometimes called have brought a major improvement to Li-ion batteries by bringing unprecedented safety, power, and cyclability. The only property for which the $LiFePO_4$ battery does not rank first is the energy density, but it is not an obstacle, even for the most demanding applications, since it is sufficient to make a 85-kW h battery that powers the Tesla S Sedan electric car, insuring a range of 300 miles per charge, for instance. The decrease of the size of the $LiFePO_4$ particles to the nano-scale has been an important factor to allow them to take over the world. The reduction in size has some trivial effects that are not specific to this material and

are a benefit in any battery, such as the increase in effective interface with the electrolyte and reduction of the path that the electrons and $Li^+$ ions have to travel inside the particles. However, the reason for the major improvement brought to the electrochemical performance upon decrease of the size to the nanosize range with $LiFePO_4$ is mainly due to the one-dimensional nature of the ionic transport specific to the olivine structure. Extended defects such as grain boundaries or other defects can block entire channels through which the $Li^+$ ions pass, or at least severely reduce their mobility. An increase in the size of the particles means a longer path through which the $Li^+$ ions have to travel to reach the surface, and thus a larger probability to collide with such defects. Another feature is the Fe—C affinity that makes easy the nano-painting of the particles with a 3 nm-thick conductive carbon layer, which solved the problem of the electronic conductivity and antisite impurities.

Second, the particles referred as nanoparticles and used in commercial batteries are few tens of nm, and there are arguments telling that there is no interest in decreasing the size of the particles further. The quantum effects are thus negligible since they would modify the intrinsic properties only for sizes $d < 10$ nm. The modification of the properties upon reduction in size mainly comes from the surface effects. Indeed, these effects are more important than usual because of some features specific to this material. In particular, the bare (non carbon-coated) $LiFePO_4$ particles have a disordered surface layer about 3 nm thick, and the fraction of atoms in this disordered layer becomes important upon decreasing $d$. The structural disorder stabilizes the solid solution $Li_xFePO_4$, so that the electrochemical properties of the part of the particle inside the surface layer are different from the core region since the Li transfer in the well-crystallized part operates by a two-phase process. Indeed, this two-phase process implies that the kinetics of the lithiation—delithiation operate by the motion of an interface between Li-rich and Li-poor phases. This two-phase process is more efficient than the solid solution reaction in $LiFePO_4$, because the coherent motion of Li-ions inside well-formed channels is not blocked by the interface. Fortunately, the nano-painting with carbon is done at a temperature that re-crystallizes the surface layer; consequently, C-$LiFePO_4$ particles are well crystallized to the surface, at least for sizes $d \geq 35$ nm. The characteristic length of the self-organization of the two-phase system suggests that the two-phase regime may not be stable for a particle size lower than 35 nm. There are, however, very few data available for such small particles. In practice, the success of $LiFePO_4$ also comes from the fact that the cathode elements are always C-$LiFePO_4$ composites, irrespective of the size of the particles that are used. Some size effects, though very small, may also have important effects. In particular, at equilibrium, the open circuit voltages of nanoparticles and bulk particles in the two-phase regime are 3.428 V and 3.420 V *vs*. $Li^+/Li$, respectively. This 8 mV difference is indeed very small, but it has sizeable effects on the voltage profile when the powder has a wide particle-size distribution. The performance and behavior of the nano-$LiFePO_4$ batteries then depend not only on the size of the particles, on their intrinsic quality (which requires a specific quality control), but also on the heterogeneity in the size distribution. This last parameter has been underestimated until recently [32], and explains probably some discrepancy between different results published on the electrochemical properties of $LiFePO_4$ and misunderstandings about the insertion/deinsertion process.

Third, the nano-$LiFePO_4$ cathode is usually coupled with a graphite anode. It provides to the anode an energy density that is one order of magnitude larger than that of the cathode, and its low voltage with respect to $Li^+/Li$ and the control of the solid-electrolyte interface (SEI) contributes to make it the best choice to have the highest energy density. Any gain in energy density that might be gained by replacing graphite by another material (nano-silicon for instance) will then be marginal. Nevertheless, graphite is presently limiting the power density of the nano-$LiFePO_4$ battery, and it also limits its cyclability. To increase the power density, the graphite has to be replaced by an element that offers a fast charge and discharge process without deterioration, which implies a material that is robust and does not suffer dilatation upon Li-insertion (exactly the opposite of nano-Si, even in nanorod or sponges). In addition, the material should not form a resistive SEI layer. The material that has these properties is $Li_4Ti_5O_{12}$. In addition, the insertion/deinsertion process is also a two-phase process like that of $LiFePO_4$. Again, it is now possible to obtain C-$Li_4Ti_5O_{12}$ composite nanoparticles. The cells equipped with C-$LiFePO_4$ particles as the cathode and C-$Li_4Ti_5O_{12}$ particles as the anode, with size 90 nm for the two powders, show remarkable results as they retain capacity up to 40C rate without aging over thousands of cycles. The drawback, however, is a loss of the energy density, because $Li_4Ti_5O_{12}$ operates at the potential 1.55 V *vs.* $Li^+/Li$, which has to be subtracted from the 3.4 V of $LiFePO_4$. The choice of the anode will then depend on the application that is targeted, requiring either more power or more energy density.

Fourth, many efforts are being made all over the world to try to find a solution to increase the energy density. Different technologies have been subject of intense research for 40 years, *e.g.* Li—air or Li—S batteries. Despite the huge financial support of all agencies across the world due to the expectation of a jump of the energy density, still these batteries show small capacity retention and low power, so that it is difficult to predict if they will ever work; at least, it is unlikely that this can be developed at a commercial level before a decade. Nevertheless, a jump by a factor two in the energy density might come from the application of nanosheet technology to the Li-ion batteries. The development of graphene and transitional metal oxide nanosheets has been pursued on the basis of fundamental scientific interest, but also with the wide potential for many technological applications. In this framework, the development of ultrathin nanosheet-structured $Li_2MSiO_4$ cathode materials has proved that the flexibility gained by this structure makes possible reversible two-Li-ion capacity with stable cyclic performance impossible to obtain otherwise. This is then a route to explore for the cathode materials that, like silicates, have two Li ions per formula that can in principle participate to the electrochemical properties, since only one Li ion was participating so far in other geometries, due to the important changes in volume and local strains implied by the extraction/insertion of the second ion. Nevertheless, at the end, the question will be on the feasibility to prepare many tons of these truly nano-structured materials such as nanosheets to prepare batteries for electric vehicles at a reasonable price. Therefore, the progress expected on the batteries provided on the market for the next years to come will presumably be only continuous.

The new synthesis of multi-composite particles is a promising route to explore in view of the results already obtained with the recent shell of carbon coated $LiFePO_4$ on top of $LiMnPO_4$ and $LiMn_{1.5}Ni_{0.5}O_4$, because the C-$LiFePO_4$ shell not only protects the core against degradation in contact with the electrolyte, but it is also an active element participating to the capacity of the cells. The working potential of $LiMnPO_4$ is 4.1 V *vs.* $Li^+/Li$; that of $LiMn_{1.5}Ni_{0.5}O_4$ is 4.7 V. These voltages are, however, only one step toward the 5 V cells that everybody would like to have, because any change in a cell impacts the other components of the battery in terms of corrosion, stability of the electrolyte, SEI layer, which have to be solved, without omitting safety concern.

If the limit in energy density comes from the cathode, the limit in power density rather comes from the anode. In this respect, the nano-$Li_4Ti_5O_{12}$ anode coupled to nano C-$LiFePO_4$ has already shown that high power can be reached with batteries working at

24C rate. The choice of this anode is detrimental to the energy density because of the redox potential of the spinel; but still, the energy density is much larger than that of a supercapacitor, and such cells will find a market. Actually, the tests have shown that the time needed to charge C-$LiFePO_4$ batteries prepared with nano-sized particles for electric and hybrid cars is not intrinsic to the batteries, but is only limited by the electric power that can be provided to the users without destabilizing the grid (typically the order of 50 kW).

## Acknowledgments

JBG thanks the Robert A. Weld Foundation for financial support. KZ thanks Hydro-QuÈbec and BATT–DOE (USA) for financial support.

## References

[1] K. Ozawa, Solid State Ionics 69 (1994) 212–221.
[2] H.J. Bang, H. Joachin, H. Yang, K. Amine, J. Prakash, Journal of the Electrochemical Society 153 (2006) A731–A737.
[3] G. Pistoia, M. Pasquali, L.A. de Picciotto, M.M. Thackery, Solid State Ionics 28 (1988) 879–885.
[4] A.K. Padhi, K.S. Nanjundaswamy, J.B. Goodenough, Journal of the Electrochemical Society 144 (1997) 1188–1194.
[5] France Innovation Scientifique & Transfert SA, FIST SA, Assessment of the State of Lithium Metal Phosphate ($LiMPO_4$) Patents (2010).
[6] U.S. Patent No. 5,910,382 and U.S. Patent No. 6,514,640 on behalf of the University of Texas System Board of Regents.
[7] H. Joachin, T.D. Kaun, K. Zaghib, J. Prakash, Journal of the Electrochemical Society 156 (2009) A401–A406.
[8] K. Zaghib, J. Dubé, A. Dallaire, K. Galoustov, A. Guerfi, M. Ramanathan, A. Benmayza, J. Prakash, A. Mauger, C.M. Julien, Journal of Power Sources 219 (2012) 36–44.
[9] K. Zaghib, M. Dontigny, A. Guerfi, P. Charest, I. Rodrigues, A. Mauger, C.M. Julien, Journal of Power Sources 196 (2011) 3949–3954.
[10] M.B. Armand, in: D.W. Murphy, J. Broadhead, B.C.H. Steel (Eds.), Materials for Advanced Batteries, Plenum, New York, 1980, p. 145. Steel (Ed.), Plenum, New York, 1980, p. 145.
[11] T. Nagaura, K. Tozawa, Progress in Batteries and Solar Cells 9 (1990) 209–215.
[12] J.R. Dahn, T. Zheng, Y. Liu, J.S. Xue, Science 270 (1995) 590–593.
[13] K.T. Lee, J. Cho, Nano Today 6 (2011) 28–41.
[14] Z.H. Chen, J.R. Dahn, Journal of the Electrochemical Society 149 (2002) A1184–A1189.
[15] N. Ravet, J.B. Goodenough, S. Besner, M. Simoneau, P. Hovington, M. Armand, in: Proceedings of the 196th Electrochemical Society Meeting, vols. 99–102, 1999, Abst. 127.
[16] B. Jin, Q. Jiang, in: Greger R. Dahlin, et al. (Eds.), Lithium Batteries, Research, Technology, Nova Science Publishers, Inc., 2009, ISBN 978-1-60741-722-4.
[17] C.M. Julien, A. Mauger, K. Zaghib, Journal of Materials Chemistry 21 (2011) 9955–9968.
[18] A. Yamada, H. Koizumi, S. Nishimura, N. Sonoyama, R. Kanno, M. Yonemura, T. Nakamura, T. Kobayashi, Nature Materials 5 (2006) 357–360.
[19] T. Maxisch, F. Zhou, G. Ceder, Physical Review B 73 (2006) 104301–104306.
[20] M.S. Islam, D.J. Driscoll, C.A. Fischer, P.R. Slater, Chemistry of Materials 17 (2005) 5085–5092.
[21] S. Nishimura, G. Kobayashi, K. Ohoyama, R. Kanno, M. Yashima, A. Yamada, Nature Materials 7 (2008) 707–711.
[22] F. Zhou, C.A. Marianetti, M. Cococcioni, D. Morgan, G. Ceder, Physical Review B 69 (2004) 201101–201105 (R).
[23] G. Chen, X. Song, T.J. Richardson, Electrochemical Solid-State Letters 9 (2006) A295–A301.
[24] V. Srinivasan, J. Newman, Journal of the Electrochemical Society 151 (2004) 1517–1529.
[25] L. Laffont, C. Delacourt, P. Gibot, M. Yue Wu, P. Kooyman, C. Masquelier, J.M. Tarascon, Chemistry of Materials 18 (2006) 5520–5529.
[26] A. Yamada, H. Koizumi, N. Sonoyama, R. Kanno, Electrochemical and Solid-State Letters 8 (2005) A409–A413.
[27] Y.Z. Dong, L. Wang, S.L. Zhang, Y.M. Zhao, J.P. Zhou, H. Xie, J.B. Goodenough, Journal of Power Sources 215 (2012) 116–121.
[28] Y.Z. Dong, H. Xie, J. Song, M. Xu, Y. Zhao, J.B. Goodenough, Journal of the Electrochemical Society 159 (2012) A1–A4.
[29] M. Xu, unpublished.
[30] C.V. Ramana, A. Mauger, F. Gendron, C.M. Julien, K. Zaghib, Journal of Power Sources 187 (2009) 555–564.
[31] C. Delmas, M. Maccario, L. Croguennec, F. Le Cras, F. Weill, Nature Materials 7 (2008) 665–671.
[32] K.T. Lee, W.H. Kan, L.F. Nazar, Journal of the American Chemical Society 131 (2009) 6044–6045.
[33] J. Maier, Nature Materials 4 (2005) 805–815.
[34] M. Wagemaker, W.J.H. Borghols, F.M. Mulder, Journal of the American Chemical Society 129 (2007) 4323–4327.
[35] J. Jamnik, J. Maier, Journal of Physical Chemistry and Chemical Physics 5 (2003) 5215–5220.
[36] N. Meethong, H.Y.S. Huang, W.C. Carter, Y.M. Chiang, Electrochemical and Solid-State Letters 10 (2007) A134–A138.
[37] R. Malik, M. Bazant, G. Ceder, Nano Letters 10 (2010) 4123–4127.
[38] B. Kang, G. Ceder, Nature 458 (2009) 190–193.
[39] A.V. Churikov, A.V. Ivanishchev, I.A. Ivanishcheva, V.O. Sycheva, N.R. Khasanov, E.V. Antipov, Electrochimica Acta 55 (2010) 2939–2950.
[40] T. Azib, S. Ammar, S. Nowak, S. Lau-Truing, H. Groult, K. Zaghib, A. Mauger, C.M. Julien, Journal of Power Sources 217 (2012) 220–228.
[41] C.A.J. Fisher, V.M. Hart Prieto, M.S. Islam, Chemistry of Materials 20 (2008) 5907–5915.
[42] P. Axmann, C. Stinner, M. Wolfahrt-Mehrens, A. Mauger, F. Gendron, C.M. Julien, Chemistry of Materials 21 (2009) 1636–1644.
[43] C.M. Julien, A. Mauger, K. Zaghib, A. Vijh, Materials science for energy storage, in: Lectures of the Workshop on Materials Science, 18–22 Jan. 2010, Chennai, India.
[44] M.L. Trudeau, D. Laul, R. Veillette, A.M. Serventi, K. Zaghib, A. Mauger, C.M. Julien, Journal of Power Sources 196 (2011) 7383–7394.
[45] C.H. Chen, J.T. Vaughey, A.N. Jansen, D.W. Dees, A.J. Kahaian, T. Goacher, M.M. Thackeray, Journal of the Electrochemical Society 148 (2001) A102–A104.
[46] K. Zaghib, A. Mauger, J. Goodenough, F. Gendron, C.M. Julien, Chemistry of Materials 19 (2007) 3740–3747.
[47] K. Zagib, M. Dontigny, A. Guerfi, J. Trottier, J. Hamel-Paquet, K. Galoutov, P. Hovington, A. Mauger, H. Groult, C.M. Julien, Journal of Power Sources 216 (2012) 192–200.
[48] K. Zaghib, A. Mauger, F. Gendron, C.M. Julien, Chemistry of Materials 20 (2008) 462–469.
[49] M. Tang, H.-Y. Huang, N. Meethong, Y.-H. Kao, W.C. Carter, Y.-M. Chiang, Chemistry of Materials 21 (2009) 1557–1571.
[50] Y.-H. Kao, M. Tang, N. Meethong, J. Bai, W.C. Carter, Y.-M. Chiang, Chemistry of Materials 22 (2010) 5845–5855.
[51] N. Meethong, Y.-H. Kao, M. Tang, H.-Y. Huang, W.C. Carter, Y.-M. Chiang, Chemistry of Materials 20 (2008) 6189–6198.
[52] K. Zaghib, M. Dontigny, P. Charest, J.F. Labrecque, A. Guerfi, M. Kopec, A. Mauger, F. Gendron, C.M. Julien, Journal of Power Sources 185 (2008) 698–710.
[53] G. Kobayashi, S. Nishimura, M. Park, R. Kanno, M. Yashima, T. Ida, A. Yamada, Abs. no. 628 PRIME 2008 Meeting, Honolulu, USA.
[54] K. Zaghib, M. Dontigny, P. Charest, J.F. Labrecque, A. Guerfi, M. Kopec, A. Mauger, F. Gendron, C.M. Julien, Journal of Power Sources 195 (2010) 8280–8288.
[55] T.L. Hill, Thermodynamics of Small Systems, W.A. Benjamin, New York, 1963.
[56] G. Ceder, L. Wang, A. Belcher, Y. Lee, K. Kang, PRIME 2008 Meeting, Honolulu, USA, Abs. no. 627.
[57] M. Wagemaker, D.P. Singh, W.J.H. Borghols, U. Lafont, L. Haverkate, V.K. Peterson, F.M. Mulder, Journal of the American Chemical Society 133 (2011) 10222–10228.
[58] C. Delacourt, P. Poizot, S. Levasseur, C. Masquelier, Electrochemical and Solid-State Letters 9 (2006) A352–A355.
[59] D. Aurbach, K. Gamolsky, B. Markovsky, G. Salitra, Y. Gofer, U. Heider, R. Oesten, M. Schmidt, Journal of the Electrochemical Society 147 (2000) 1322–1331.
[60] A. Ait-Salah, A. Mauger, C.M. Julien, F. Gendron, Materials Science and Engineering B 129 (2006) 232–244.
[61] N. Ravet, M. Gauthier, K. Zaghib, A. Mauger, J. Goodenough, F. Gendron, C. Julien, Chemistry of Materials 19 (2007) 2595–2602.
[62] Y. Hu, M.M. Doeff, R. Kostecki, R. Finones, Journal of the Electrochemical Society 151 (2004) A1279–A1285.
[63] C.M. Julien, A. Mauger, A. Ait-Salah, M. Massot, F. Gendron, K. Zaghib, Ionics 13 (2007) 395–411.
[64] C.M. Julien, K. Zaghib, A. Mauger, M. Massot, A. Ait-Salah, M. Selmane, F. Gendron, Journal of Applied Physics 100 (2006) 63511–63518.
[65] K. Rissouli, K. Benkhouja, J.R. Ramos-Barrado, C.M. Julien, Materials Science and Engineering B 98 (2003) 185–189.
[66] D.W. Choi, D.H. Wang, I.T. Bae, J. Xiao, Z.M. Nie, W. Wang, V.V. Viswanathan, Y.J. Lee, J.G. Zhang, G.L. Graff, Z.G. Yang, J. Liu, Nano Letters 10 (2010) 2799–2805.
[67] D. Wang, H. Buqa, M. Crouzet, G. Deghenghi, T. Drezen, I. Exnar, N.-H. Kwon, J.H. Miners, L. Poletto, M. Grâtzel, Journal of Power Sources 189 (2009) 624–628.
[68] S.K. Martha, B. Markovski, J. Grinblat, Y. Gofer, O. Haik, E. Zinigrad, D. Aurbach, T. Drezen, D. Wang, G. Deghenghi, I. Exnar, Journal of the Electrochemical Society 156 (2009) A541–A552.
[69] S.-M. Oh, S.-W. Oh, C.-S. Yoon, B. Scrosati, K. Amine, Y.-K. Sun, Advanced Functional Materials 20 (2010) 3260–3265.
[70] Y.S. Choi, S. Kim, S.S. Choi, J.S. Han, J.D. Kim, S.E. Jeon, B.H. Jung, Electrochimica Acta 50 (2004) 833–835.
[71] S. Kuroda, N. Tobori, M. Sakuraba, Y. Sato, Journal of Power Sources 119–121 (2003) 924–928.
[72] W. Xing, S.Z. Qiao, R.G. Ding, F. Li, G.Q. Lu, Z.F. Yan, H.M. Cheng, Carbon 44 (2006) 216–224.

[73] Q. Zhang, G. Peng, G. Wang, M. Qu, Z.L. Yu, Solid State Ionics 180 (2009) 698–702.
[74] Z. Bakenov, I. Taniguchi, Journal of the Electrochemical Society 157 (2010) A430–A436.
[75] Z. Bakenov, I. Taniguchi, Solid State Ionics 176 (2005) 1027–1034.
[76] Z. Bakenov, I. Taniguchi, Journal of Power Sources 195 (2010) 7445–7451.
[77] S.-M. Oh, H.-G. Jung, C.S. Yoon, S.-T. Myung, Z. Chen, K. Amine, Y.-K. Sun, Journal of Power Sources 196 (2011) 6924–6928.
[78] S.-M. Oh, S.W. Oh, S.-T. Myung, S.-M. Lee, Y.-K. Sun, Journal of Alloys and Compounds 506 (2010) 372–376.
[79] M. Yonemura, A. Yamada, Y. Takey, Y. Sonoyama, R. Kanno, Journal of the Electrochemical Society 151 (2004) A1352–A1356.
[80] M. Piana, B.L. Cushing, J.B. Goodenough, N. Penazzi, Solid State Ionics 175 (2004) 233–237.
[81] A. Yamada, S.C. Chung, Journal of the Electrochemical Society 148 (2001) A960–A967.
[82] A. Yamada, Y. Kudo, K.-Y. Liu, Journal of the Electrochemical Society 148 (2001) A1153–A1158.
[83] A. Yamada, Y. Takei, H. Koizumu, N. Sonoyama, R. Kanno, Chemistry of Materials 18 (2006) 804–813.
[84] N. Amdouni, K. Zaghib, F. Gendron, A. Mauger, C. Julien, Ionics 12 (2006) 117–126.
[85] M. Kopec, A. Yamada, G. Kobayashi, S. Nishimura, R. Kanno, A. Mauger, F. Gendron, C.M. Julien, Journal of Power Sources 189 (2009) 1154–1163.
[86] K. Zaghib, M. Trudeau, A. Guerfi, J. Trottier, A. Mauger, R. Veillette, C.M. Julien, Journal of Power Sources 204 (2012) 177–181.
[87] S. Oh, S. Myung, J. Park, B. Scrosati, K. Amine, Y. Sun, Pacific Rim Meeting on Electrochemical and Solid-State Science (PRIME), Honolulu, 2012, extended abstract 777.
[88] Y. Lu, J. Shi, Z. Guo, Q. Tong, W. Huang, B. Li, Journal of Power Sources 194 (2009) 786–793.
[89] D.Y. Wang, Z.X. Wang, X.J. Huang, L.Q. Chen, Journal of Power Sources 146 (2005) 580–583.
[90] Y. Zhang, C.S. Sun, Z. Zhou, Electrochemistry Communications 11 (2009) 1183–1186.
[91] L. Daniel, S. Martinet, T. Gutel, G. Bourbon, E. Radvanyi, M. Amuntencei, S. Patoux, Pacific Rim Meeting on Electrochemical and Solid-State Science (PRIME), Honolulu, 2012, extended abstract 709.
[92] M. Minakshi, P. Singh, Pacific Rim Meeting on Electrochemical and Solid-State Science (PRIME), Honolulu, 2012, extended abstract 381.
[93] X.J. Wang, X.Q. Yu, H. Li, X.Q. Yang, J. McBreen, X.J. Huang, Electrochemistry Communications 10 (2008) 1347–1350.
[94] S.Y. Chung, J.T. Bloking, Y.M. Chiang, Nature Materials 1 (2002) 123–128.
[95] N. Ravet, A. Abouimrane, M. Armand, Nature Materials 2 (2003) 702.
[96] P.S. Herle, B. Ellis, N. Coombs, L.F. Nazar, Nature Materials 3 (2004) 147–152.
[97] M. Wagemaker, B.L. Ellis, D. Lützenkirchen-Hecht, F.M. Mulder, L.F. Nazar, Chemistry of Materials 20 (2008) 6313–6315.
[98] S.Y. Chung, J.T. Bloking, Y.M. Chiang, Nature Materials 2 (2002) 702–703.
[99] H. Wang, W.-D. Zhang, L.-Y. Zhu, M.-C. Chen, Solid State Ionics 178 (2007) 131–136.
[100] W.-S. Kim, S.-B. Kim, I.C. Jang, H.H. Lim, Y.S. Lee, Journal of Alloys and Compounds 492 (2010) L87–L90.
[101] K. Amine, H. Tukamoto, H. Yasuda, Y. Fujita, Journal of Power Sources 68 (1997) 604–608.
[102] Q. Zhong, A. Bonakdarpour, M. Zhang, Y. Gao, J.R. Dahn, Journal of the Electrochemical Society 144 (1997) 205–214.
[103] J. Liu, A. Manthiram, Chemistry of Materials 21 (2009) 1695–1707.
[104] D. Liu, J. Trottier, P. Charest, J. Fréchette, A. Guerfi, A. Mauger, C.M. Julien, K. Zaghib, Journal of Power Sources 204 (2012) 127–132.
[105] R.A. Huggins, Pacific Rim Meeting on Electrochemical and Solid-State Science (PRIME), Honolulu, 2012, extended abstract 707.
[106] D. Pasero, N. Reeves, V. Pralong, A.R. Westt, Journal of the Electrochemical Society 155 (2008) A282–A291.
[107] R.V. Chebiam, F. Prado, A. Manthiram, Chemistry of Materials 12 (2001) 2951–2957.
[108] S. Venkatraman, A. Manthiram, Chemistry of Materials 14 (2002) 3907–3912.
[109] A. Nyten, A. Abouimrane, M. Armand, T. Gustaffson, J.O. Thomas, Electrochemistry Communications 7 (2005) 156–160.
[110] K. Zaghib, A. Ait-Salah, N. Ravet, A. Mauger, F. Gendron, C.M. Julien, Journal of Power Sources 160 (2006) 1381–1386.
[111] R. Dominko, M. Bele, M. Gaberscek, A. Meden, M. Remska, J. Jamnik, Electrochemistry Communications 8 (2006) 217–222.
[112] Y. Chung, S. Yu, M.S. Song, S.-S. Kim, W. Il Cho, Bulletin of the Korean Chemical Sociey 32 (2011) 4205–4209.
[113] Y.-L. Xiao, Z.-L. Gong, Y. Yang, Journal of Power Sources 174 (2007) 528–532.
[114] R. Dominko, Journal of Power Sources 184 (2008) 462–468.
[115] D. Rangappa, K.D. Murukanahally, T. Tomai, A. Unemoto, I. Honma, Nano Letters 12 (2012) 1146–1151.
[116] C. Ling, D. Banerjee, W. Song, M. Zhang, M. Matsui, Journal of Materials Chemistry 22 (2012) 13517–13523.
[117] http://www.me.utexas.edu/news/2011/0711_goodenough_hydro-quebec.php.